Enhancing the Per-Unit-Length Data Density in Near-Field Chipless-RFID Systems with Sequential Bit Reading

Jaroslav Havlicek, Cristian Herrojo, *Member, IEEE*, Ferran Paredes, *Member, IEEE*, Javier Mata-Contreras, and Ferran Martín, *Fellow, IEEE*

***Abstract*— In this paper, a novel near-field chipless-RFID system with sequential bit reading is reported. The main novelty concerns the tags, implemented by means of straight half-wavelength resonators separated a small distance and forming a linear chain in the direction orthogonal to their axis. By this means, the number of resonant elements (or bits) per unit length of the tag is significantly increased, as compared to previous implementations, with the result of very competitive tags in terms of data density. The active part of the reader is a microstrip line loaded with a shunt stub. Through a proper design, it is possible to achieve a significant excursion of the transmission coefficient when the stub is either loaded or unloaded with a functional resonant element of the tag. Consequently, by tag motion over the reader (stub), it is possible to infer the ID code by simply injecting a harmonic signal to the input port of the stub-loaded line (the ID code is contained in the amplitude modulated, AM, signal at the output port). This system has been validated by considering 100-bit tags exhibiting a surface data density of 4.9 bits/cm^2. However, the relevant parameter is the data density per unit length, as high as 16.7 bit/cm, i.e., much larger than previous values reported in the literature in similar chipless-RFID systems.**

***Index Terms* — Chipless-RFID, microstrip, half-wavelength resonator, secure paper.**

I. Introduction

A novel chipless-RFID concept where tags are read by proximity (through near-field) and sequentially was recently reported [1]-[3]. The main advantage of this time-domain approach, of special interest for secure paper applications, is the data storage capability, only limited by tag size. As compared to time-domain reflectometry (TDR) based tags [4],[5], spectral signature barcodes [6]-[9], or tags exploiting hybrid coding techniques [10]-[14], the proposed time-domain based tags are implemented by printing all-identical resonators at equidistant positions forming a linear chain [2]. Coding (programming) is achieved by detuning (cutting) certain resonant elements and it has been demonstrated that tag erasing is also possible by simply short-circuiting those previously detuned resonant elements [2].

The interrogation signal is a harmonic signal tuned to the frequency of the resonant elements of the tag, f_0 (or close to it), and tag reading proceeds by displacing the tag over a dedicated transmission line fed by the interrogation signal. Through tag motion, the amplitude of the feeding signal is modulated by the coupling between the line and the functional tag resonators, and the ID code is contained in the envelope function present at the output port of the line (which can be inferred by means of an envelope detector). The system works similar to an amplitude modulator (AM), where the carrier signal is the interrogation signal and modulation is achieved by tag motion (Fig. 1). Similar to spectral signature barcodes, the envelope function exhibits dips, or peaks, providing the ID code, but in time domain. For this reason, we can designate these chipless-RFID tags as time-domain signature barcodes. Since the spectral bandwidth is virtually null, it follows that the number of bits is only limited by tag size, proportional to the number of bits.

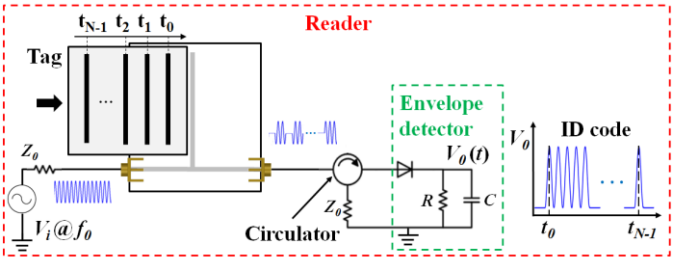

Fig. 1. Illustration of the working principle of the proposed chipless-RFID system. In a reading operation, the tag is displaced at short distance over the reader through a mechanical guiding system providing tag/reader alignment.

Although a figure of merit of chipless-RFID tags is usually the data density per area unit, in these chipless-RFID tags based on linear chains of resonant elements, the relevant parameter is the number of bits per unit length. The reason is that the shape factor of the tag is very extreme, and the number of bits is typically limited by tag length, rather than

This work was supported in part by MINECO-Spain under Project TEC2016-75650-R, in part by Generalitat de Catalunya (project 2017SGR-1159), in part by the Institució Catalana de Recerca i Estudis Avançats (who awarded F. Martín), and in part by FEDER funds. The work of C. Herrojo was supported by MINECO through the FPI under Grant BES-2014-068164. The work of J. Havlicek was supported by Czech Science Foundation and Czech Technical University in Prague through projects 17-02760S and SGS16/226/OHK3/3T/13, respectively.

J. Havlicek is with the Department of Electromagnetic Field, Czech Technical University in Prague, Technicka 2, 16627 Prague, Czech Republic.

J. Havlicek C. Herrojo, F. Paredes, and F. Martín are with GEMMA/CIMITEC (Departament d'Enginyeria Electrònica), Universitat Autònoma de Barcelona. 08193 BELLATERRA (Barcelona), Spain. E-mail: Ferran.Martin@uab.es.

J. Mata-Contreras is with the Departamento de Ingeniería de Comunicaciones, Escuela Técnica Superior de Ingeniería de Telecomunicación, Universidad de Málaga, 29071 Málaga, Spain.

width. In [1]-[3], by using split ring resonators (SRRs), a per-unit-length data density of 3 bits/cm was achieved. In this paper, a novel tag (and reader) with much higher density of information per unit length (i.e., 16.7 bit/cm) is reported and validated. The tags are based on straight half-wavelength resonators, and the reader is a 50 Ω transmission line loaded with an open shunt stub.

II. Proposed Chipless-RFID Tags and Reader

The active part of the reader is a stub-loaded microstrip line, implemented on the *Rogers RO3010* substrate with thickness h = 0.635 mm and dielectric constant ε_r = 10.2 [Fig. 2(a)]. This structure exhibits a stop band response, with transmission zeros at the frequency where the electrical length of the open stub is 90º and at its odd harmonics (Fig. 3). By etching a straight half-wavelength resonator in a different substrate, and locating it on top of the stub, as Fig. 2(b) illustrates, the response of the structure is modified as depicted in Fig. 3, where two transmission zeros in the vicinity of the fundamental (first) resonance of the stub-loaded line appear (frequency splitting). Note that the half wavelength resonator can be tuned to operate at different frequencies, not necessarily at the fundamental frequency of the stub-loaded line. The response for the half-wavelength resonator tuned to the second resonance is also included in Fig. 3. It can be seen that it is possible to achieve frequency splitting in the vicinity of any of the stub resonances.

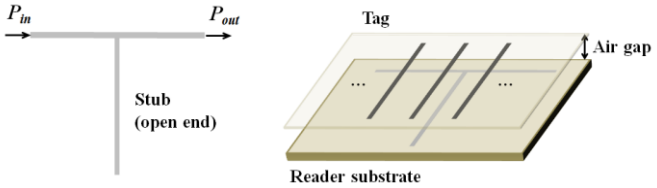

Fig. 2. Layout of the active part of the reader (a) and 3D view of the loaded reader with one of the half-wavelength resonators of the tag aligned with the reader stub (b). The length and width of the stub are 26 mm and 0.2 mm, respectively. The width of the transmission line is 0.6 mm (50 Ω line). The separation between adjacent resonators in the tag chain is 0.2 mm and resonator dimensions are 34 mm × 0.4 mm (so that the tag period is 0.6 mm). The tag chain has been implemented on the *Rogers RO4003C* substrate with thickness h = 0.2 mm and dielectric constant ε_r = 3.55.

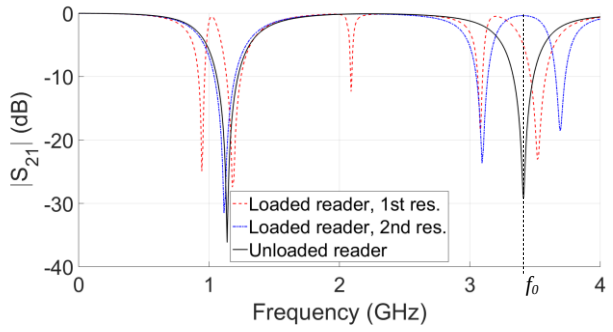

Fig. 3. Magnitude of the transmission coefficient (S_{21}) of the unloaded reader and reader loaded with a single half-wavelength resonator perfectly aligned. For the loaded reader, two different cases have been considered in regard to the half-wavelength resonator, i.e., either tuned at the first (fundamental) or second resonance of the stub. The considered air gap is 0.3 mm. These results have been inferred by electromagnetic simulation, using *Keysight Momentum*.

After an exhaustive analysis, we have concluded that the preferred option to implement the chipless-RFID system is to tune the half-wavelength resonators in the vicinity of the second resonance of the stub. The reason is that the effects of multiple couplings between the stub and the tag resonators are less severe by tuning the system at this frequency, as compared to working in the vicinity of the fundamental frequency (where glitches that appear in the response, not shown, may prevent from a correct and robust tag reading, unless the tag period is substantially increased).

For tag and reader design, we have tuned the dimensions in order to achieve the response shown in Fig. 3 corresponding to resonator tuning at the second resonance. Maximum transmission at the second resonance, f_0, of the unloaded line can be appreciated when a half-wavelength resonator is perfectly aligned with the stub. By this means, a significant excursion of the transmission coefficient is expected by tuning the interrogation signal to that frequency (f_0 = 3.47 GHz) or close to it (a convenient situation in order to obtain a high modulation index and hence clearly discern between the two logic states).

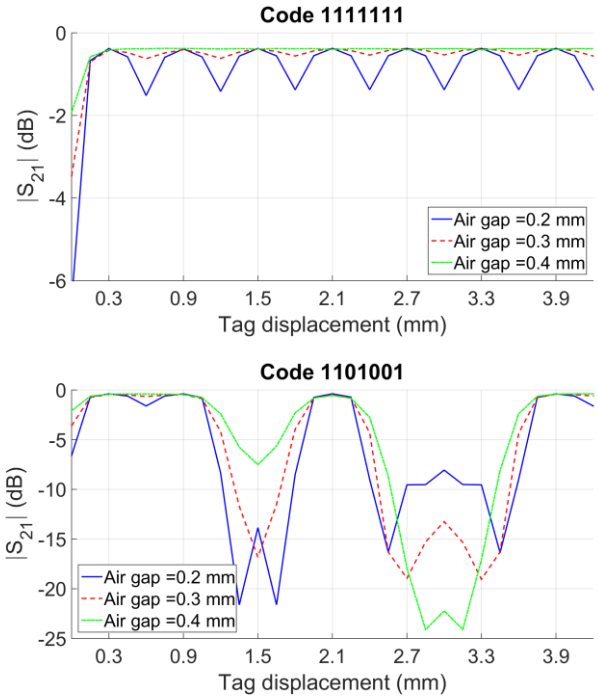

Fig. 4. Variation of the transmission coefficient at the interrogation signal frequency that results from a relative displacement between the tag and the reader for the indicated codes. Several air gaps are considered.

Fig. 4 depicts the variation of the transmission coefficient at the frequency of the interrogation signal, set to f_0, as a 7-bit tag is displaced above the reader. Two different bit combinations, indicated in the figure, have been considered, in order to validate, at simulation level, the proposed system. An important aspect is the robustness against air gap variations. Therefore, we have repeated the simulations of the considered 7-bit tags for air gaps of 0.2 mm and 0.4 mm (the nominal air gap being 0.3 mm). The corresponding responses are also included in Fig. 4, and it can be appreciated that differences

with the air gap variation arise. These differences are caused by frequency shift of the second resonance of the stub as a result of the air gap variation, and are mainly manifested by a different level of the transmission coefficient when a detuned resonator is on top of the reader stub. Nevertheless, for all bit combinations, the responses exhibit the expected behavior. Namely, for a logic state '1', corresponding to the presence of a functional resonator on top of the stub, maximum transmission is achieved; conversely, when the half-wavelength resonator is detuned (i.e., not functional) by cutting it, corresponding to the logic state '0', the transmission coefficient is severely reduced. Note, therefore, that, as compared to papers [1]-[3], we use negative logic in this paper.

III. Experimental Validation

To experimentally validate the proposed system, we have fabricated a 100-bit tag by means of standard photo-etching, where all-functional resonators have been etched. Conversely, the reader has been fabricated by means of a *LPKF HF-100* drilling machine (the photographs are depicted in Fig. 5). We have then read this tag by means of the set-up present in our laboratory, described in [1], consisting of a function generator, an envelope detector and an oscilloscope (to display the time domain response of the tag, i.e., the AM signal containing the ID code), plus the mechanical guiding system. The measured envelope is depicted in Fig. 6, where it can be seen that dips are not present, as long as all bits are set to '1'. Then we have detuned some resonant elements by cutting them (hence setting some bits to '0'), and the measured normalized envelope reveals the presence of such '0' states (as dips in the time-domain responses). Thus, tag programming can be simply done by cutting the required resonant elements, similar to [1], [2]. Note that three codes have been programmed, as it is visible in Fig. 6, and in all the cases such codes have been correctly read.

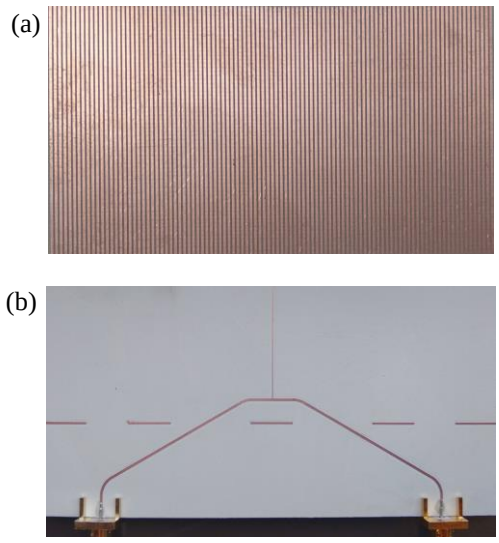

Fig. 5. Photograph of the fabricated 100-bit tag with all bits set to the logic state '1' (a), and reader (b). The space occupied by the tag is 60 mm × 34 mm. Line bending in the feeding lines of the reader has been applied in order to reduce the coupling between the tag resonators and the feeding lines.

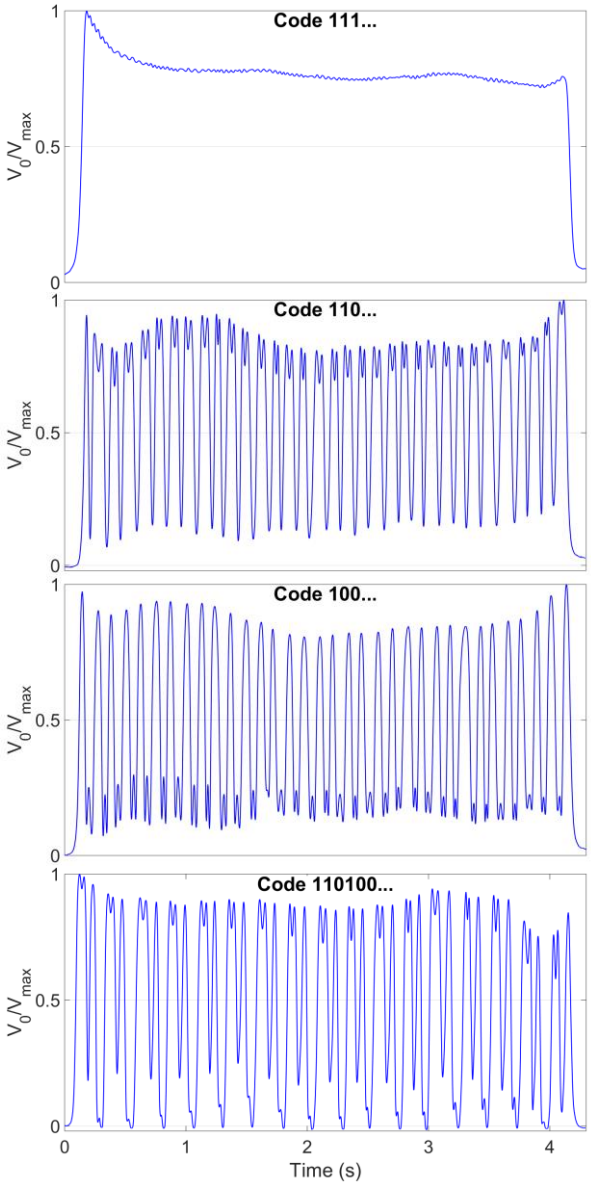

Fig. 6. Measured normalized envelope for the 100-bit tags with the indicated codes. For each code, the repeating period is shown. The reason of the variation of the maximum voltage in the figures is related to the fact that absolute uniformity in the gap space between the tag and the reader cannot be guaranteed.

IV. Discussion

The surface information density of the tag is 4.9 bit/cm^2 (not as good as the one reported in [1]-[3], i.e., 8.9 bit/cm^2), but, most important, we have accommodated 100 bits in a length of 60 mm, corresponding to a per-unit-length density of 16.7 bit/cm, i.e., substantially larger than the one of previous similar works based on tags implemented with split ring resonators [1]-[3]. Such high per-unit-length information density has been achieved by driving the separation of the resonant elements of the tag to the limit of the available technology (0.2 mm). Further reducing this spacing may have negative effect on tag reading due to possible couplings between the line stub (reader) and neighbor resonators in the tag. However, this aspect has not been considered as long as

for the limiting inter-resonator spacing (0.2 mm), the one considered in this work, this effect has been found to be negligible. It should be also pointed out that it is possible to reduce the width of the tag (in order to increase the data density per surface) by increasing the frequency of the interrogation signal (by this means, both the reader stub and the resonant elements of the tag can be shortened).

Finally, concerning the substrate of the tag and tag fabrication, chemical etching of a laminated microwave substrate (the one specified in the caption of Fig. 2) has been considered in this paper (mainly focused on demonstrating the potential of this new approach to enhance the density of bits per unit length). Nevertheless, it was demonstrated in [2],[3] that by replacing such tag substrates and fabrication procedure with a flexible substrate, such as paper, and inkjet printing, the functionality of the tags is preserved. Rather than the quality factor of the resonant elements, the key aspect for system functionality is the effect of coupling between the sensitive part of the reader (the stub in our case) and the resonant element of the tag. Such coupling does not depend critically on the substrate material of the tag, and for that reason the functionality is preserved in [2],[3]. It should be pointed out, however, that the quality factor of the resonant elements may have influence on the effects of neighbor resonators, if it is too low. Nevertheless, under these circumstances, the solution is to simply increase the distance between adjacent resonators. According to the period of the reported tags (0.6 mm), there is margin to proceed in that way (if necessary, depending on the considered substrate), yet keeping a significant density of bits per unit length.

V. Conclusions

In conclusion, the functionality of a time-domain near-field chipless-RFID system with tags based on a chain of linear (straight) half-wavelength resonators has been demonstrated. We have designed the tags and the reader, a stub-loaded microstrip line, and the system has been optimized for operation at f_0 = 3.47 GHz (the frequency of the interrogation signal). Programmable 100-bit chipless-RFID tags have been reported. Moreover the achieved information density per area and length (the most important one in this type of tags based on a resonator chain) is 4.9 bit/cm^2 and 16.7 bit/cm, respectively. By using the proposed system, the shape factor of the tags has been severely improved as compared to those of previous tags based on sequential bit reading.

References

[1] C. Herrojo, J. Mata-Contreras, A. Núñez, F. Paredes, E. Ramón, and F. Martín, “Near-field chipless-RFID system with high data capacity for security and authentication applications”, *IEEE Trans. Microw. Theory Techn.*, vol. 65, no. 12, pp. 5298-5308, Dec. 2017.

[2] C. Herrojo, J. Mata-Contreras, F. Paredes, A. Núñez, E. Ramon, and F. Martín, “Near-field chipless-RFID system with erasable/programable 40-bit tags inkjet printed on paper substrates”, *IEEE Microw. Wireless Compon. Lett.*, vol. 28, pp. 272-274, Mar. 2018.

[3] C. Herrojo, M. Moras, F. Paredes, A. Núñez, E. Ramón, J. Mata-Contreras, F. Martín, “Very low-cost 80-bit chipless-RFID tags inkjet printed on ordinary paper”, *Technologies*, vol. 6, p. 52, 2018.

[4] F.J. Herraiz-Martínez, F. Paredes, G. Zamora, F. Martín, J. Bonache, “Printed magnetoinductive-wave (MIW) delay lines for chipless RFID applications”, *IEEE Trans. Ant. Propag*., vol. 60, pp. 5075-5082, Nov. 2012.

[5] M. Schüßler, C. Damm, M. Maasch, and R. Jakoby, “Performance evaluation of left-handed delay lines for RFID backscatter applications,” *IEEE MTT-S Int. Microw. Symp*. 2008, Atlanta, USA, pp. 177-180.

[6] S. Preradovic, I. Balbin, N. C. Karmakar, and G. F. Swiegers, "Multiresonator-based chipless RFID system for low-cost item tracking," *IEEE Trans. Microw. Theory Techn*., vol. 57, pp. 1411-1419, May 2009.

[7] A. Vena, E. Perret, and S. Tedjini, “High-capacity chipless RFID tag insensitive to the polarization”, *IEEE Trans. Ant. Propag*., vol. 60, pp. 4509-4515, Oct. 2012.

[8] R. Rezaiesarlak and M. Manteghi, "Complex-natural-resonance-based design of chipless RFID tag for high-density data," *IEEE Trans. Ant. Propag*., vol. 62, pp. 898-904, Feb. 2014.

[9] M. Polivka, J. Havlicek, M. Svanda, J. Machac, “Improvement in robustness and recognizability of RCS response of U-shaped strip-based chipless RFID tags”, *IEEE Ant. Wirel. Propag. Lett*., vol 15, pp. 2000-2003, 2016.

[10] A. Vena, E. Perret, S. Tedjini, "Chipless RFID tag using hybrid coding technique," *IEEE Trans. Microw. Theory Techn*., vol. 59, pp. 3356-3364, Dec. 2011.

[11] M. A. Islam and N. C. Karmakar, "A novel compact printable dual-polarized chipless RFID system," *IEEE Trans. Microw. Theory Techn*., vol. 60, pp. 2142-2151, Jul. 2012.

[12] S. Genovesi, F. Costa, A. Monorchio, G. Manara, “Chipless RFID tag exploiting multifrequency delta-phase quantization encoding”, *IEEE Ant. Wireless Propag. Lett*., vol. 15, pp. 738-741, 2015.

[13] O. Rance, R. Siragusa, P. Lemaître-Auger, E. Perret, "Toward RCS magnitude level coding for chipless RFID," *IEEE Trans. Microw. Theory Techn*., vol. 64, pp. 2315-2325, Jul. 2016.

[14] C. Herrojo, F. Paredes, J. Mata-Contreras, S. Zuffanelli and F. Martín, “Multi-state multi-resonator spectral signature barcodes implemented by means of S-shaped Split Ring Resonators (S-SRR)”, *IEEE Trans. Microw. Theory Techn*., vol. 65, pp. 2341-2352, Jul. 2017.